Thermochimica Acta 371 (2001) 121–126

thermochimica acta

www.elsevier.com/locate/tca

The non-isothermal devitrification of glasses in the $CaO{\cdot}4GeO_2$–$SrO{\cdot}4GeO_2$ composition range

M. Catauro*, A. Marotta

Department of Materials and Production Engineering, University Federico 11 Piazzale Tecchio, 80125 Napoli, Italy

Received 18 October 2000; accepted 12 December 2000

Abstract

The effect of replacing CaO by SrO on the glass transition temperature and on devitrification behaviour in a series of glasses in the calcium tetragermanate–strontium tetragermanate composition range has been studied by differential thermal analysis (DTA), X-ray diffraction (XRD) and Fourier-transform infrared (FTIR) spectra. A similar GeO_4/GeO_6 molar ratio was found in all the glasses of the series. The progressive replacing of CaO by SrO caused a decrease of the glass transition temperature. All glasses studied exhibited internal crystal nucleation. The crystallizing phases were identified as $CaGe_4O_9$ and $SrGe_4O_9$. No solid solutions occur in glass containing both CaO and SrO. The effect of the specific surface of the glass samples on devitrification processes has been studied.

Keywords: Devitrification; Glass transition temperature; Alkaline earth germanate

1. Introduction

The properties of binary M_2O–GeO_2 and MO–GeO_2 glasses have been extensively studied [1–6]. Phase equilibria in the binary germanate system have been also reported [7]. On the other hand, very little is known about the ternary germanate glasses. This paper is part of a research programme with the aim of filling this gap.

In previous papers [8–12] the effect on glass transition temperature and devitrification behavior of the progressive substitution of an alkaline oxide M_2O by another M'_2O oxide in tetragermanate glasses were discussed. The substitution of M_2O by M'_2O causes the value of the glass transition temperature to go through a minimum at a molar ratio $M_2O/M'_2O = 1$ according to the "mixed alkali effect". The structures of all the studied glasses contain GeO_4 and GeO_6 groups in nearly the same molar ratio. In the lithium–sodium tetragermanate glasses a ternary compound $LiNaGe_4O_9$ was found among the crystallizing phases [8]. The stability of the lithium–potassium tetragermanate glasses increases with the increase of difference between crystallizing phases and mother glass composition [9]. In the sodium–potassium tetragermanate glasses solid solutions between $Na_4Ge_9O_{20}$ and $K_4Ge_9O_{20}$ crystallize [10]. In the strontium–barium tetragermamate glasses solid solution between $SrGe_4O_9$ and $BaGe_4O_9$ were found crystallize in glass containing both SrO and BaO [11]. In the calcium–barium tetragermanate glasses the crystallizing phase were $CaGe_4O_9$ and $BaGe_4O_9$ [12]. The devitrification behavior of ternary tetragermanate glasses containing

---

* Corresponding author. Tel.: +39-81-768-2415;
fax: +39-81-758-2595.
E-mail address: catauro@unina.it (M. Catauro).

PII: S0040-6031(00)00784-X

Ba^{2+} and Pb^{2+} ions in 3/1, 1/1 and 1/3 molar ratios, has been also studied [13]. Glasses with 3/1 and 1/1 Ba^{2+}/Pb^{2+} molar ratio are phase separated and devitrify in two steps. Bulk crystallization of Ge_4O_9 is followed at higher temperatures by GeO_2 crystals growth on the surface of the samples. The glass with 1/3 Ba^{2+}/Pb^{2+} molar ratio devitrifies into a solid solution of $BaGe_4O_9$ and $PbGe_4O_9$ crystals.

In the present work the effect of a progressive replacement of CaO by SrO, on the structure, the glass transition temperature and the devitrification behavior of tetragermanate glasses were studied by Fourier-transform infrared spectroscopy (FTIR), differential thermal analysis (DTA) and X-ray diffraction (XRD).

2. Experimental

The glass compositions are expressed by the general formula

$$(1-x)\mathrm{CaO}\cdot x\mathrm{SrO}\cdot 4\mathrm{GeO_2}$$

with $x = 0.00$; 0.25; 0.50; 0.75; 1.00. In the course of the paper each glass is named by the corresponding x value. The glasses were prepared by mixing appropriate quantities of ultra pure calcium carbonate (Aldrich), strontium carbonate (Aldrich) and germanium oxide (Heraeus) in a batch sized to yield 3 g of glass. The glasses were melted in an uncovered Pt crucible in an electric oven. The crucible containing the glass was weighed both before and after the glass was removed. The weight of the glass agreed with that anticipated from the batch calculation. This result indicates that the actual glass composition is close to that based on the glass batch. The melts were quenched by plunging the bottom of the crucible into cold water. Although this resulted in fracture of the glass, for all the compositions pieces of transparent glass of size sufficient for the experimental measurements were obtained by this technique.

Fourier-transform infrared (FTIR) absorption spectra were recorded in the 4000–400 cm^{-1} range using a Mattson 5020 system, equipped with a DTGS KBr (deuterated triglycine sulfate with potassium bromide windows) detector. A spectral resolution of 2 cm^{-1} was chosen. Each test sample was mixed with KBr (1 wt.% of former) in an agate mortar, and then pressed into 200 mg pellets of 13 mm diameter. The spectrum for each sample represents an average of 20 scans, which were normalized to the spectrum of the blank KBr pellet. The FTIR spectra have been analyzed by a Mattson software (FIRST Macros).

DTA curves were recorded in air at a heating rate of 10°C/min on bulk or fine powdered (<45 μg) specimens (about 50 mg) from room temperature to 900°C. A Netzsch thermoanalyser high temperature DSC 404 was used with Al_2O_3 as reference material. The experimental error in DTA temperature is ± 1°C. The DTA curves have been elaborated by a Netzsch software.

The amorphous nature of the glasses and the identification of the phases crystallizing in the glass during the DTA runs were ascertained by XRD using a Philips diffractometer. Powders of each glass sample were scanned from $2\Theta = 5°$ to $60°$ using Cu Kα radiation.

3. Results and discussion

Fig. 1 shows the infrared transmission spectra of the as-quenched glasses in the 400–1200 cm^{-1} range where the Ge–O–Ge and O–Ge–O stretching and deformation modes are actives. The two strongest absorption peaks lie at about 750 and 570 cm^{-1}.

From previous studies [4], it is known that in the infrared spectra of hexagonal and vitreous GeO_2, in which the coordination number of germanium is 4, the absorption band, due to the Ge–O–Ge stretching lies at 878 cm^{-1}, while in tetragonal GeO_2, in which germanium assumes six-fold coordination, this band occurs at 688 cm^{-1}. In alkali germanate the coordination number of Ge atoms changes from 4 to 6 with the addition of alkali oxide to GeO_2 glass and this band progressively shifts towards lower wavenumbers values [4].

The spectra of Fig. 1 exhibit near the same shift of this band as shown in Table 1. This result suggests a similar GeO_4/GeO_6 molar ratio in all the glasses of the series. The absorption band at about 550 cm^{-1} may be related to mixed stretching–bending vibrations of GeO_4 tetrahedra [14].

Fig. 2 shows the DTA curves of the five as-quenched glasses recorded on bulk samples. A slope change followed by an exothermic peak occurs on all curves. The slope change may be attributed to the

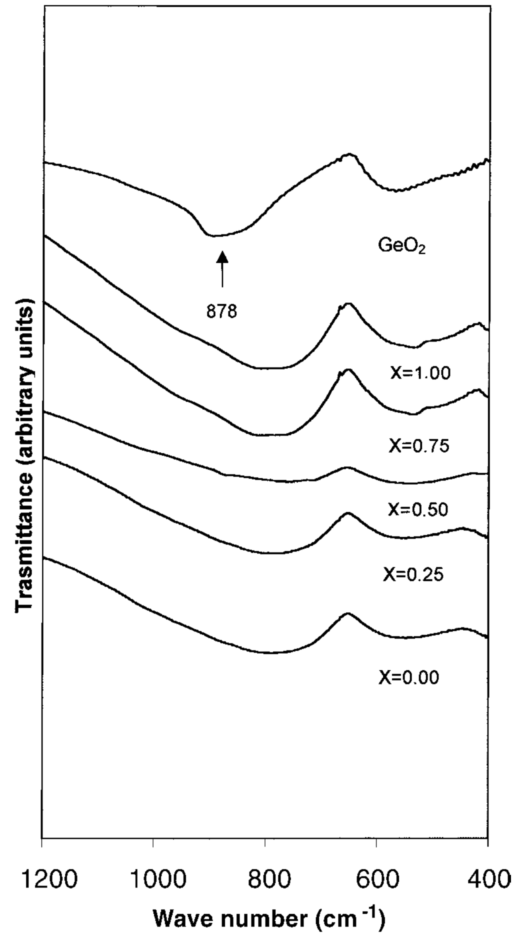

Fig. 1. Fourier-transform infrared spectroscopy (FTIR) transmittance spectra for glasses of composition $(1-x)CaO \cdot xSrO \cdot 4GeO_2$.

glass transition. In this work, the extrapolated onset of the slope change was taken (Fig. 3) as the glass transition temperature (T_g). The values of T_g for the five investigated glasses are reported in Table 1.

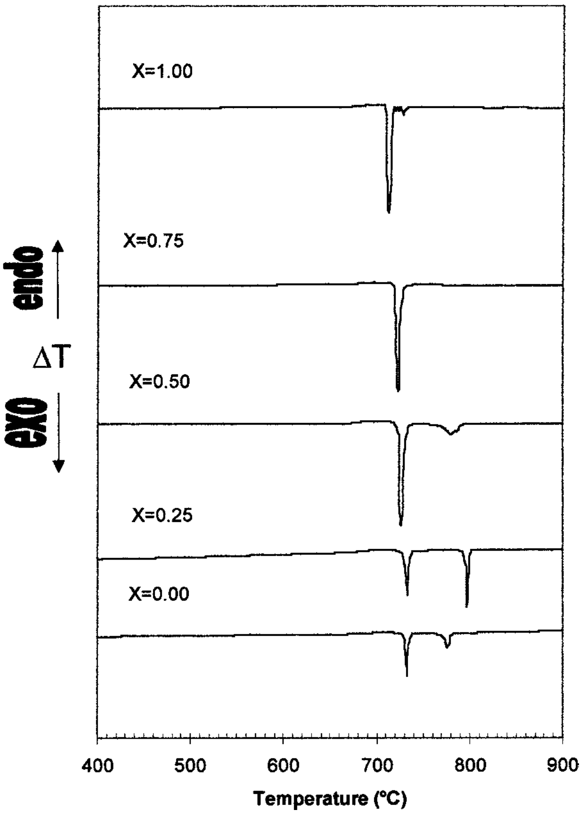

Fig. 2. DTA curves recorded at $10^\circ C\,min^{-1}$ for glasses of composition $(1-x)CaO \cdot xSrO \cdot 4GeO_2$.

According to Ray [15], the effect of any cation on T_g is related to the following factors: (i) reduction in density of covalent cross-linking; (ii) change in oxygen density of the network; (iii) number and strength of the cross-links between oxygen and the cation. In the glasses studied the O/Ge ratio is constant (i.e. $O/Ge = 2.25$) and the GeO_4/GeO_6 molar ratio

Table 1
DTA and IR data for glasses of composition $(1-x)CaO \cdot xSrO \cdot 4GeO_2$[a]

Glasses	T_g (°C)	T_{p1} (°C)	T_{p2} (°C)	ν_1 (cm^{-1})	ν_2 (cm^{-1})	Activation energy, E ($kJ\,mol^{-1}$)
$x = 0.00$	688	730 [729]	800	756	577	686
$x = 0.25$	670	732 [731]	797	748	575	727
$x = 0.50$	669	725 [725]	779	747	569	701
$x = 0.75$	665	721 [720]		754	576	654
$x = 1.00$	664	710 [707]		756	577	758

[a] T_g: glass transition temperatures; T_p: DTA peak temperatures of bulk samples [in square brackets of powdered samples]; ν_1 and ν_2: frequencies of the two strongest intensity bands in crystallized samples.

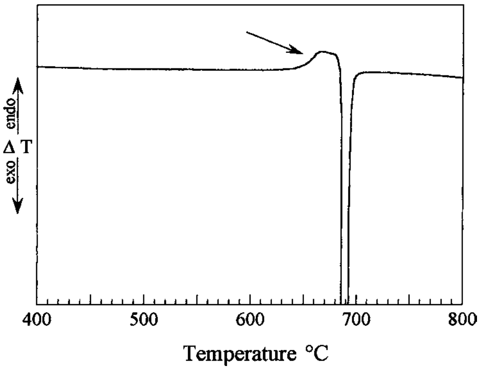

Fig. 3. DTA curve of the term $x = 0.00$ shown on expanded ordinate scale to well display the slope change attributed to the glass transition.

is the same, therefore, the cross-link density does not change. The strength and the number of the cross-links between oxygen and the cations are related to the coordination number and to the radius and of the cations. The coordination number is 8 for both cations. The M–O strength is reduced as a result of the larger radii of Sr^{2+} (1.30 Å) compared with Ca^{2+} (1.14 Å). Therefore, the progressive replacing of Ca^{2+} by Sr^{2+} causes the decrease of the glass transition temperature.

Nucleation in glass-forming systems can occur either in the volume or on the surface of the sample. In practice, surface crystal nucleation occur more easily and is observed in most compositions. To achieve internal crystal nucleation it is often necessary to add nucleating agents. However, certain glass systems nucleate internally without such additions. The total number of nuclei (N) per unit volume is the sum of surface nuclei (N_s) of homogeneous bulk nuclei (N_b) formed during the DTA run and heterogeneous bulk nuclei N_c [16]. The value of N_s, N_b and N_c are proportional to the specific surface area of the samples, the reciprocal of the DTA heating rate and the amount of nucleating agent, respectively. The higher the number of N, the lower the temperature of the DTA crystallization peak is [17]. Moreover, the shape of the DTA crystallization peak is strongly affected by the crystallization mechanism [18], to surface and bulk crystallization correspond broad and sharp peaks, respectively.

In the studied glasses no nucleating agent was added ($N_c = 0$). The sharp shape of the crystallization peaks on the DTA curves, carried out on bulk samples (low specific surface area), Fig. 2, suggests that in all glasses studied internal crystal nucleation is dominant $N_b \gg N_s$. To confirm this hypothesis DTA curves were also recorded on very fine powdered samples. No appreciable differences of the temperature (T_p) (see Table 1), and the shape of the crystallization peak were found. Taking into account the great increase of the number of surface nuclei due to the high specific surface area of the very fine powdered samples this result indicates that the specific surface area of the samples has not influence on the devitrification process of these glasses and surface crystallization compared with bulk nucleation can be neglected.

To ascertain the amorphous nature of the glasses and to identify the phases crystallizing during the DTA runs, XRD measurements were carried out on the as-quenched glasses and on samples subjected to a DTA run from room temperature to the temperature of each DTA exo-peak.

The XRD patterns of the as-quenched glasses show broad humps characteristic of their amorphous state.

The XRD patterns of samples of the glasses heated to the temperature of the first DTA peak exhibit (Fig. 4) several sharp reflections that were all assigned to $CaGe_4O_9$ (JCPDS file 14-515) and $SrGe_4O_9$ (JCPDS file 14-29) crystals.

The difftactograms obtained for the terms $x = 0.00$, 0.25 and 0.50 heated above both the crystallization exothermic peaks (Fig. 5) exhibit a high number of sharp lines that all correspond to $CaGe_4O_9$ crystals (JCPDS file 14-515).

For a range of simple substitutional solid solution to form, there are certain requirements that must be met. First, the ions that replace each other must have the same charge. Second, the ions that are replacing each other must be fairly similar in size. From a review of the experimental result on metal alloy formation, it has been suggested that a difference of 15% in the radii of the metal atoms that replace each other is the most that can be tolerated if a substantial range of substitutional solid solution is to form.

Then, ions of very similar size substitute for each other easily and extensive solid solution form which are stable at all temperatures; the enthalpy of mixing of such similar-sized ions is likely to be small and the driving force for solid solution, formation is the increased entropy. With ions that differ in size by 15–20%, solid solution may form, especially at high

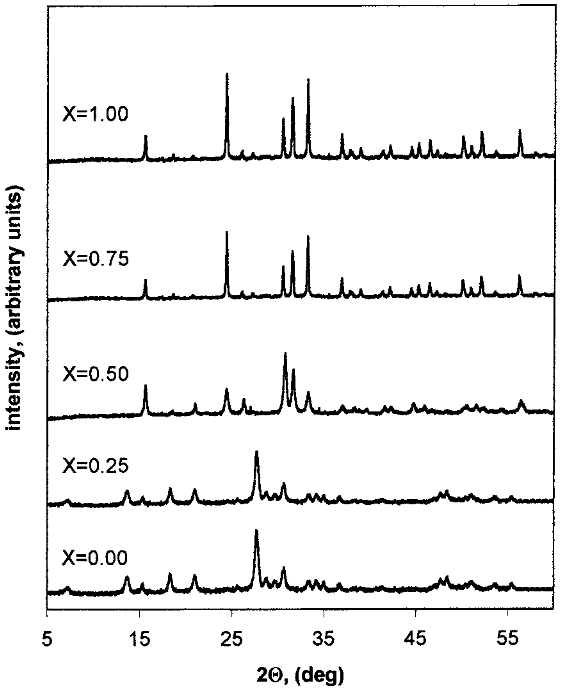

Fig. 4. X-ray diffraction (XRD) patterns for glasses of composition $(1-x)CaO{\cdot}xSrO{\cdot}4GeO_2$ heated until the temperature of the first DTA exo-peak.

temperature where the entropy solid solution is able to offset the significant positive enthalpy term. In considering whether or not solid solutions form, an important factor is the crystal structure of the two-end members. In the systems that exhibit complete ranges of solid solution, it is clearly essential that the two end members be isostructural. The reverse is not necessarily true, however, and just because two phase are isostructural, it does not follow that they will form solid solutions with each other.

The XRD patterns of the crystallizing phases in terms of the series shown in Fig. 4 suggest that the two phases are isostructural but the solid solutions is not formed.

Table 2
Crystallizing phase $(1-x)CaO{\cdot}xSrO{\cdot}4GeO_2$[a]

$(1-x)CaO{\cdot}xSrO{\cdot}4GeO_2$	Crystallizing phase
$x = 0.00$	$CaGe_4O_9$
$x = 0.25$	$CaGe_4O_9$
$x = 0.50$	$CaGe_4O_9$ $SrGe_4O_9$ (tc)
$x = 0.75$	$SrGe_4O_9$
$x = 1.00$	SrG_4O_9

[a] tc: trace.

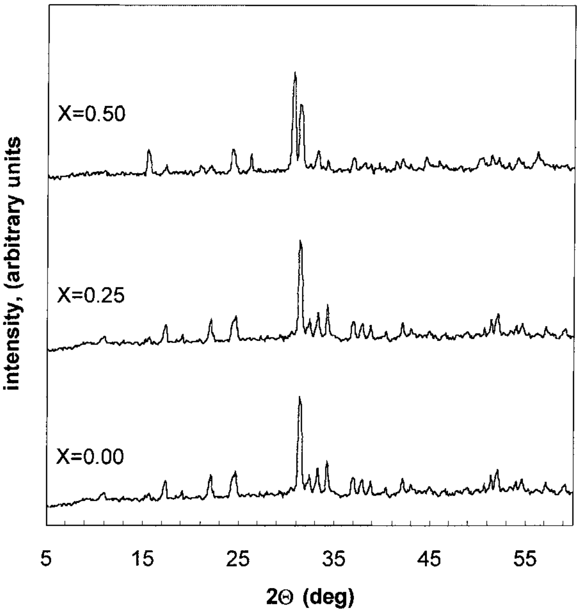

Fig. 5. X-ray diffraction (XRD) patterns of the term $x = 0.00$, $x = 0.25$ and $x = 0.50$ heated until the temperature of the second DTA exo-peak.

The crystallizing phase during the DTA runs are reported in Table 2.

The activation energy E, for crystallization was evaluated from the DTA curves using the equation [19]

$$\ln\beta = -\left(\frac{E}{R}\right)\left(\frac{1}{T_p}\right) + \text{const}$$

This equation is based on the temperature shift of DTA peak T_p as the DTA heating rate β is changed. Multiple DTA runs were recorded in air at different heating rates on bulk samples of the studied glasses. Plots of $\ln\beta$ against $1/T_p$ give straight lines in all cases. The value of activation energy calculation calculated from their slope, reported in Table 1, differ from each other less than the experimental error ±10%.

4. Conclusions

From the experimental results the following conclusions can be drawn.

1. The structures of the devitrified glasses contain GeO_4 and GeO_6 in the same molar ratio.
2. The progressive replacing of CaO by SrO causes a progressive decrease of the glass transition temperature.
3. All glasses exhibit internal crystal nucleation.
4. The crystallizing phase are $CaGe_4O_9$ and $SrGe_4O_9$. No solid solution were found.
5. The activation energy of crystal growth is near the same in all glasses.

References

[1] K.S. Evstropiev, A.O. Iivanov, in: F.R. Matson, G.E. Rindone (Eds.), Advances in Glass Technology. Part 2. Plenum Press, New York, 1963, p. 79.

[2] M.K. Murty, J. Ip, Nature (London) 201 (1964) 3285.

[3] J.E. Shelby, J. Am. Ceram. Soc. 57 (1974) 436.

[4] M.K. Murthy, E.M. Kirby, Phys. Chem. Glasses 5 (1964) 144.

[5] S. Sakka, K. Kamiya, J. Non-Cryst. Solids 49 (1982) 103.

[6] H. Verweij, J.H.J. M Buster, J. Non-Cryst. Solids 34 (1979) 81.

[7] E.M. Levin, C.R. Robins, H.C. McMurdie, Phase Diagrams for Ceramists, American Ceramic Society, Columbus, OH, 1964, p. 93.

[8] M. Catauro, A. Aronne, P. Pemice, A. Marotta, J. Mater. Sci. Lett. 15 (1996) 817.

[9] G. Laudisio, M. Catauro, J. Eur. Ceram. Soc. 18 (1998) 359.

[10] G. Laudisio, M. Catauro, Mater. Chem. Phys. 51 (1997) 54.

[11] M. Catauro, G. Laudisio, J. Thermal Anal. Calorimetry 58 (1998) 617–623.

[12] M. Catauro, S. Gargano, G. Laudisio, Thermochim. Acta 356 (2000) 127–131.

[13] G. Laudisio, M. Catauro, Phys. Chem. Glasses 39 (1998) 62.

[14] K.E. Lipinska-Kalita, J. Non-Cryst. Solids 119 (1990) 41.

[15] N.H. Ray, J. Non-Cryst. Solids 15 (1974) 423.

[16] A. Maroffa, A. Buri, F. Branda, Thermochim. Acta 40 (1980) 397.

[17] A. Marotta, A. Buri, F. Branda, J. Mater. Sci. 16 (1981) 341.

[18] W.W. Wendlandt, Thermal Analysis, Wiley, New York, 1986, p. 448.

[19] T. Ozawa, Kinetics of non-isothermal crystallization, Polymer (1971) 150–158.